ELSEVIER

Journal of Power Sources 97–98 (2001) 702–710

JOURNAL OF POWER SOURCES

www.elsevier.com/locate/jpowsour

A new method to study Li-ion cell safety: laser beam initiated reactions on both charged negative and positive electrodes

J.P. Pérès[a,*], F. Perton[a], C. Audry[a], Ph. Biensan[a], A. de Guibert[a], G. Blanc[b], M. Broussely[c]

[a]*SAFT, Direction de la Recherche, 111, Boulevard Alfred Daney, 33074 Bordeaux, France*
[b]*CETHIL-INSA, 20, Avenue Albert Einstein, 69621 Villeurbanne, France*
[c]*SAFT, BP 1039, 86060 Poitiers, France*

Received 23 June 2000; accepted 29 January 2001

Abstract

The improvement of Li-ion batteries safety in abuse use is one of the key issues for their establishment in future hybrid or electrical vehicles. Such a challenge requires a perfect understanding of phenomena which could occur in abuse situation. A new technique for a better understanding of Li-ion cell safety has been so investigated. Reactions between electrolyte and charged electrodes (positive and negative just recovered from dismantled charged 4/5A cells) have been initiated by a laser beam, having a monitored intensity and time pulse. From such a device, a strong and controlled heating can be generated, in a very short time scale, on a defined electrode surface area. This localized heating, which is supposed to be similar to that could occur from a cell internal short-circuit, is able to initiate ''self-propagation reactions'' on charged negative and positive electrodes. This new technique has allowed a ranking of charged electrodes in terms of ''self-propagation ability''. This range of new data has been compared to results obtained from classical thermal characterization methods (DSC, DTA) and results obtained from normalized abuse tests. Global charged negative and positive electrodes degradation mechanisms have been proposed in good agreement with the whole results. The safety of a done Li-ion cell seems mainly related to active negative and positive active materials, but also to other components of the electrodes, and especially additive carbons and aluminum collector of the positive side. © 2001 Elsevier Science B.V. All rights reserved.

Keywords: Li-ion; Safety; Reaction propagation; Laser

1. Introduction

Rechargeable lithium batteries have many intrinsic advantages, such as, high voltage and high energy density [1–4]. However, the improvement of their safety is still one of the key issues for the establishment of such batteries, especially for industrial applications, as hybrid and electrical vehicle [5]. Safety of Li-ion has now to be certified in ''abuse use'', even for large cells. It must be noted that the safety of small consumer cells has only been achieved with a carefully designed cell safety features [6].

Li-ion cells safety is tightly linked to the unstability of charged positive or negative electrodes, in presence of liquid electrolyte. Many publications are relative to the evaluation of thermal stability of positive or negative materials by DSC experiments [7], or to the whole cell behavior during abusive tests at charged state [8].

Not so much studies focusing on reactivity of whole single positive or negative electrodes have been reported so far. The aim of this study is to evaluate the reactivity of a given positive or negative electrode, just recovered from dismantled Li-ion cells at charged state.

The reactivity of a charged electrode must be considered in terms of ''thermal stability in presence of electrolyte'', but also in terms of ''ability to self-propagation''.

Indeed, self-propagation on charged electrodes is a key factor to a better understanding of the occurrence or not of Li-ion cells thermal runaway in abuse use.

The thermal unstability of Li-ion cells is linked to the thermal metastability of negative and positive electrodes, and to the occurrence of the liquid electrolyte. The electrodes thermal metastabilty increases as the end charge voltage increases. The exothermic reactions which can occur between charged electrodes and electrolyte can lead to important heat generation in the cell. Abuse conditions (over charge, short-circuits, operation at high temperatures, ...) accelerate the rate of heat generation. Indeed, heat genera-

* Corresponding author. Tel.: +33-557-10-6886; fax: +33-557-10-6877.
E-mail address: jean-paul.peres@saft.alcatel.fr (J.P. Pérès).

0378-7753/01/$ – see front matter © 2001 Elsevier Science B.V. All rights reserved.
PII: S0378-7753(01)00731-5

tion increases exponentially with temperature, while heat dissipation only increases linearly. Insufficient heat dissipation can cause thermal runaway, with failure of the cell, flames and smokes.

As a consequence, specific safety tests, which are supposed to be representative of abnormal events that may occur in abuse use, have been developed to evaluate the level of safety of a done Li-ion cell, with a done electrochemical definition. The most recognized ones have been edited by Underwriters Laboratories (UL), United Nations (UN) for transportation and International Electrochemical Commission (IEC) [8]. Japan storage Battery Association (JBA) has proposed specific tests for lithium batteries, widely followed today.

Among the battery of possible tests [8], the so-called nail test (pass from side to side a charged cell by a nail of specified dimensions), initially proposed by the JBA, is able to simulate an internal short-circuit.

2. Experimental

2.1. Impact of the cell electrochemical definition on nail tests results

Laboratory 4/5A cells with different positive and negative electrodes have been realized in order to evaluate the impact of the jelly roll definition on charged cell safety.

The electrochemical characteristics of the cell are the following:

- capacity ≈0.45 Ah;
- separator: cellgard (microporous);
- $LiPF_6$-based electrolyte;
- stainless steel can with glass to metal seal (GTMS);
- positive electrode: aluminum collector/active material/additive carbons/PVDF;
- negative electrode: Cu collector/active material/binders;
- after an optimized formation, the 4/5A cells have been charged (with floating) at required voltage values (between 3.6 and 4.2 V). Nail tests have been performed on charged cells (nail of 3 mm diameter at 3 cm/s rate). Temperature increase, weight loss and macroscopic phenomena (venting, flames, smokes) have been studied carefully. The test is considered as ''succeeded'' for a ''B11'' or a ''B21'' final test criterion (Table 1).

2.2. Thermal analysis of charged positive electrodes

Lithium coin cells have been made with positive electrodes (different positive active materials/additive carbons/PVDF), using a $LiPF_6$-based electrolyte. Electrochemical cycling was made on a Mac Pile apparatus (BIO-LOGIC). Positive electrodes were delithiated at constant current, and then charged at the required end charge voltage during 20 h. The charged positive electrode thermal stability has been evaluated by both DSC and DTA experiments (D50 from Shimadzu, heating rate = 10–20°C/min).

Table 1
Nail tests (end experiment characteristic criteria)

A	No explosion, no fire, no smokes, no leak			
B	No explosion, no fire, no smokes			
C	No explosion, no fire			
D	No explosion			
Criterion	1	2	3	4
Weight loss	<5%	5–12%	12–25%	>25%
Criterion	1	2	3	4
Temperature	<110°C	110–250°C	250–400°C	>400°C

2.3. Laser tests

Prototype 4/5A cells have been realized with various negative and positive electrodes definitions. These prototype cells have been especially studied to be easy dismantled, just before the laser experiment, and to allow an easy recovering of charged negative and positive electrodes in the shorter possible time.

A glove box under argon flow has been realized just under the laser beam generation, in order to perform, prototypes cells dismantling, and recovering of charged electrodes from jelly roll, under inert atmosphere.

The recovered charged electrodes have been placed on optimized stands (Plexiglas or PTFE) and irradiated by the beam of a power laser (CILAS-ALCATEL CI-4000).

The energy received by the studied charged electrode is a fraction of the total energy emitted by the laser. The whole energy losses, which could occur during the laser beam focalization can be summarized as follows (Fig. 1):

the emitted energy (E_0) is:

$$E_0 = KI\,\Delta t$$

where, K: intrinsic laser factor; I: current value; Δt: time pulse.

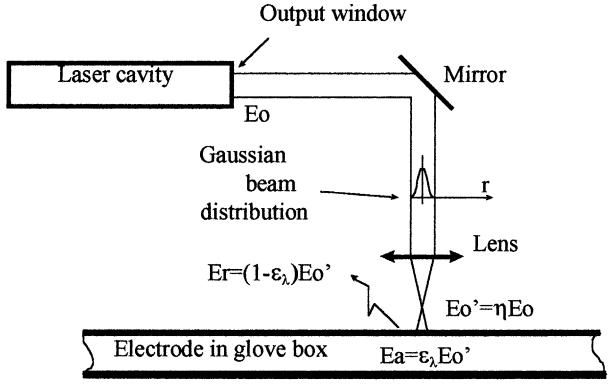

Fig. 1. Initiation of reaction propagation on Li-ion charged electrode by a laser beam. Whole energy losses during laser beam focalization.

The K factor is determined by a laser internal calorimeter, which allows the (P_0) emitted power evaluation:

$$P_0 = \frac{E_0}{\Delta t}$$

Moreover, in the beam, the energy exhibits a Gaussian repartition. A total of 99% of the power is included in a one centimeter diameter disc.

The beam is directed and focalized by a mirror and a lens. The lens allows to modify the laser beam impact size (diameter between 3 and 10 mm).

The E'_0 energy received by the studied electrode is:

$$E'_0 = \eta E_0$$

where η, a factor which depends of the used optics. For all performed experiments, $\eta = 0.83$.

At last, only a part of the incident energy is absorbed (E_a), as an other part is reflected (E_r). E_a is a function of studied electrode emissivity, in the laser wavelength range:

$$E_a = E_\lambda E'_0$$

E_λ is between 0.75 and 0.95, in function of the kind of charged studied electrode.

The local temperature increase is proportional to the absorbed energy density (absorbed energy/impact surface):

$$D_a = \frac{E_a}{ds}$$

The pristine laser power measured during the run experiment is $P_0 = 430 \pm 10$ W.

As a result: $P_0 = 360 \pm 10$ W.

2.4. Video/infrared following of the experiments

Standard and infrared videos have been realized during electrodes irradiations. They have allowed, on the one hand, to observe macroscopic phenomena (flames, smokes, ...), and, on the other hand, to have an idea of reached temperatures and speeds of front reaction propagation.

The infrared camera provides a tension V, linked to electrode surface temperature:

$$V = K\varepsilon_{\lambda_1-\lambda_2}T^4$$

where, K: intrinsic factor of the camera; $\varepsilon_{\lambda_1-\lambda_2}$: surface emissivity in the spectral ($\lambda_1 - \lambda_2$) of the camera (3.0–5.4 μm ≠ laser wavelength ($\lambda = 10.6$ μm)); T: surface temperature.

The emissivity has been fixed at one (maximum value of the "blackbody"). As a result, we can consider that the real temperature is higher than those measured.

3. Results

3.1. Impact of the cell electrochemical definition on nail tests results

The obtained results have been reported in Table 2.

First, one should have to notice that with the "carbon type 2" negative electrode definition, the reached maximum safe voltage (3.8 V) is the same than for the "carbon type 1" electrode. However, for higher end charge voltage (≥3.9 V), the observed reactions after nail penetration are more violent. This point will be discussed later.

Table 2
Nail test results on 4/5A cells with different electrochemical definitions

Test	Negative electrode	Positive electrode (active positive material)	End charge voltage (V)	Criteria
1	Carbon 1	$LiCoO_2$	4.3	B21
2	Carbon 1	$LiNi_{1-x}Co_xO_2$	3.6	B21
3	Carbon 1	$LiNi_{1-x-y}Co_xM1_yO_2$	3.8	B21
4	Carbon 1	$LiNi_{1-x-y}Co_xM1_yO_2$	3.9	C33
5	Carbon 2	$LiNi_{1-x-y}Co_xM1_yO_2$	3.8	B21
6	Carbon 2	$LiNi_{1-x-y}Co_xM1_yO_2$	3.9	D24
7	Carbon 1	$LiNi_{1-x-y}Co_xM2_xO_2$	4.2	B21
8	Carbon 1	$LiNi_{1-x-y-z}Co_xM1_yM2_zO_2$	4.2	B21

Test	Positive electrode (same additive carbons and binder)	End charge voltage (V)	Positive irreversible capacity (mAh/g)	Positive reversible capacity (mAh/g)
1	$LiCoO_2$	4.3	10	150
2	$LiNi_{1-x}Co_xO_2$	3.6	40	80
3	$LiNi_{1-x-y}Co_xM1_yO_2$	3.8	35	115
4	$LiNi_{1-x-y}Co_xM1_yO_2$	3.9	35	135
5	$LiNi_{1-x-y}Co_xM1_yO_2$	3.8	35	115
6	$LiNi_{1-x-y}Co_xM1_yO_2$	3.9	35	135
7	$LiNi_{1-x-y}Co_xM2_xO_2$	4.2	15	155
8	$LiNi_{1-x-y-z}Co_xM1_yM2_zO_2$	4.2	35	160

Table 3
Post-mortem analysis after nail tests (X-ray diffraction and X-fluorescence analysis)

Electrodes	Nail test end criteria	Far from the nail impact	On the nail impact
Nail test 5 ($LiNi_{1-x-y}Co_xM1_yO_2$)	B21	No modification of positive electrode	Small degradation of active positive material
Nail test 5 (carbon type 2)		No modification of negative electrode	Cu_2O traces
Nail test 6 ($LiNi_{1-x-y}Co_xM1_yO_2$)	D24	Degradation of active positive material, occurrence of LiF and Ni metal	No pristine active material. LiF, Ni metal (strong), no additive carbons, $LiAlO_2$ (weak). Al collector disappearance
Nail test 6 (carbon type 2)		Cu, Cu_2O, LiF, phosphates, great amount of Li_2CO_3	Cu, Cu_2O, LiF, phosphates, great amount of Li_2CO_3

For the positive side, electrodes made with $LiCoO_2$ exhibit a high thermal stability. Moreover, M1 and M2 doping of $LiNi_{1-x}Co_xO_2$ structure, has allowed to stabilize the material structure at charged state.

3.2. Post-mortem analysis after nail tests

X-ray diffraction and X-fluorescence analysis have been performed after ''failed'' or '' succeeded'' nail tests. Samples of negative and positive electrodes, recovered near and far from the nail impact, have been studied. The obtained results have been reported in Table 3.

3.3. Thermal analysis of charged positive electrodes

To a better understanding of nail tests results and corresponding post-mortem analysis, a detailed study of whole positive electrode thermal stability has been undertaken.

DTA experiments (20–1000°C) have been realized on both charged $Li_{1-t}CoO_2$ and charged $Li_{1-t}Ni_{1-x-y}Co_xM1_yO_2$-based positive electrodes, in presence of electrolyte. X-ray diffraction analysis have been also performed at intermediate temperatures (300, 600, 900°C), in order to have a better understanding of whole charged positive electrode degradation phenomena. The obtained results have been reported on Table 4.

3.4. Charged positive material thermal degradation

Delithiated $Li_{1-t}CoO_2$ and $Li_{1-t}Ni_{1-x}M_xO_2$ materials are unstable and their thermal decomposition has been reported in the literature [7].

$$Li_{1-t}(Ni_{1-x}M_x)O_2 \Rightarrow Li_{1-t}(Ni_{1-x}M_x)O_{2-t} + \tfrac{1}{2}tO_2$$

$$Li_{1-t}CoO_2 \Rightarrow \tfrac{1}{3}tCo_3O_4 + (1-t)LiCoO_2 + \tfrac{1}{3}tO_2$$

$Li_{1-t}Ni_{1-x}M_xO_2$ is a very complex solid solution which depends on de-intercalation amount $(1-t)$, and of the nature and the amount of dopants (M = Co, M1, M2, ...). As temperature increases, there is a progressive degradation of pristine lamellar character of $Li_{1-t}(Ni_{1-x}M_x)O_2$. Degradated active positive material can be first indexed as a ''pseudo $LiNi_2O_4$ spinel phase'' (300°C) and then as a ''pseudo NiO cubic phase'' (600°C), even if a large Li amount still exits in the structure.

This charged positive material thermal degradation entails an oxygen release, oxygen which is able to react with the liquid electrolyte.

Table 4
X-ray diffraction and X-fluorescence analysis performed at intermediate temperatures during (20–1000°C) positive electrode DTA analysis

20°C	300°C	600°C	900°C
$LiCoO_2$-based positive electrode			
$LiCoO_2$ additive carbons binders Al collector	$LiCoO_2$	$LiCoO_2\downarrow$	$LiCoO_2\downarrow$
	Co_3O_4	$Co_3O_4\uparrow$	$Co_3O_4\downarrow$
		CoO	CoO↑
		LiF	LiF
			$LiAlO_2$
			Co metal (weak)
	Al collector	Al collector	No Al collector
$LiNi_{1-x-y}Co_xM1_yO_2$-based positive electrode			
Active material additive carbons binders Al collector	''Spinel phase''	''Spinel phase''↓	
		''Cubic phase''	''Cubic phase''↑
		LiF	LiF
			$LiAlO_2$
	Carbons	Carbons	No carbons
			Ni metal
	Al collector	Al collector	No Al collector

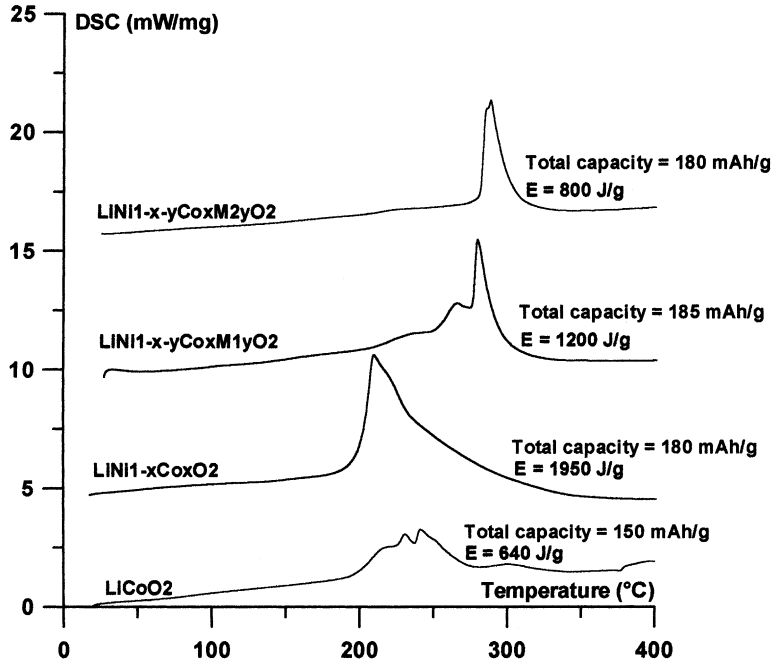

Fig. 2. Comparative DSC study of charged positive electrode with different electrochemical definitions, in presence of electrolyte.

3.5. Interaction between charged positive material and electrolyte

DSC curves (20–400°C), obtained on charged $Li_{1-t}CoO_2$, charged $Li_{1-t}Ni_{1-x}Co_xO_2$, charged $Li_{1-t}Ni_{1-x-y}Co_xM1_yO_2$, and charged $Li_{1-t}Ni_{1-x-y}Co_xM2_yO_2$ electrodes, in presence of electrolyte, have been reported on Fig. 2. The observed exothermic reaction is relative to the interaction between electrolyte and oxygen released by charged positive material degradation. There are three important parameters: the temperature reaction range, the kinetic of the reaction and the total energy of the reaction.

The obtained results demonstrate that the kinetic of the involved reaction is lower for $Li_{1-t}CoO_2$ than for $Li_{1-t}Ni_{1-x}Co_xO_2$. However, one should have to notice that the total charged capacity of the positive electrode (just before DSC experiment) is lower for $Li_{1-t}CoO_2$ than for $Li_{1-t}Ni_{1-x}Co_xO_2$ (150 mAh/g at 4.2 V versus Li against 180 mAh/g at 4.1 V versus Li).

The addition of M1 or M2 to $Li_{1-t}Ni_{1-x}Co_xO_2$ composition tends to increase strongly the thermal stability of positive material at charged state. Indeed, the involved exothermic reaction occurs in a higher temperature range and exhibits a lower total energy.

X-ray diffraction experiments, performed at intermediate temperature steps (100, 200, 250, 300 and 400°C), and coupled with TGA/MS experiments have allowed to evidence:

- a delay in intermediate "pseudo spinel" formation, and as result, a delay in oxygen release, in the case of M1 doping;
- a delay in intermediate "pseudo spinel" disappearance, and as a result, a delay in oxygen release, in the case of M2 doping.

These points will be discussed in details in an overcome paper.

3.6. Interaction between positive active material and the other components of the positive electrode

To a better understanding of charged positive electrode reactivity in the (400–1000°C) temperature range, new DTA experiments have been performed.

DTA curves (20–1000°C), obtained on mixing of:

- active material/PVDF;
- active material/additive carbons;
- active material/Al collector, have been reported on Fig. 3.

The obtained results are in good agreement with the previous X-ray diffraction experiments and allow to explain fully the degradation of the whole charged positive electrode (Tables 3 and 4).

Indeed, first, PVDF decomposition (starting at 480°C), entails the formation of LiF (positive material attack).Then, at higher temperatures ($T \approx 700$°C), the additive carbons of the positive electrode are able to reduce the degradated active positive material ("pseudo NiO cubic phase") at Ni metal state. The involved reactions are the following:

$$NiO + C \Rightarrow Ni + CO \quad \text{and} \quad NiO + CO \Rightarrow Ni + CO_2$$

At last, over 850°C, an other reaction could occur, in the

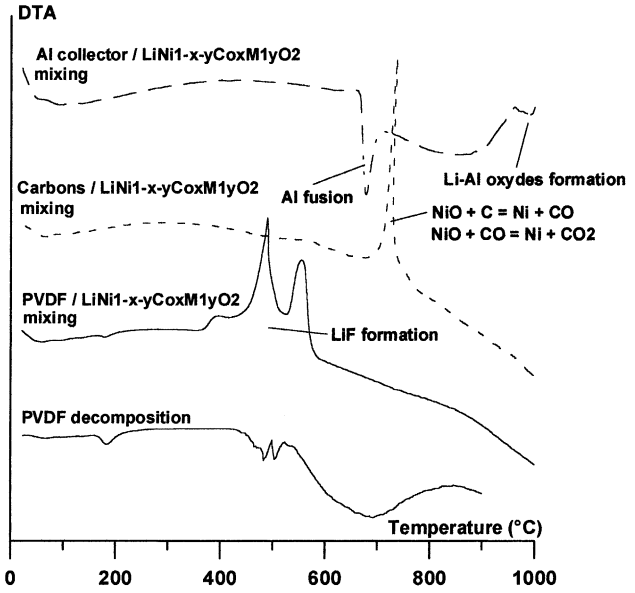

Fig. 3. DTA study: interaction between positive active material and other components of positive electrode (PVDF binder: conductive additive carbons and aluminum collector).

lithium/aluminum/oxygen system, reaction which can lead to Li–Al oxides formation.

The occurrence or not, of active material reduction at metal state by the conductive additive carbons of the positive electrode, or the aluminum collector, will be discussed an other overcome paper, especially in terms of enthalpy of reaction.

3.7. A new tool to study Li-ion cell safety: laser beam initiated reactions

The aim of this study is to evaluate the reactivity of a given positive or negative electrode, just recovered from dismantled Li-ion cells at charged state, in presence of electrolyte, by studying macroscopic propagation phenomena occurrence. Indeed, the evaluation of propagation parameters, as starting threshold, front temperatures, front rates, ... is very useful to a better Li-ion cell safety understanding, as they cannot be evaluated by DSC, ATD, ARC experiments or classic abusive tests.

Different positive and negative electrodes definitions have been investigated. The natures of positive ($LiCoO_2$, doped $LiNiO_2$, ...) and negative (carbons type 1 or 2) active materials are the main parameter which have been taken into account in the electrodes definitions.

The charged electrodes degradation reactions have been initiated by a laser beam, having a monitored intensity and time pulse. From such a device, a strong and controlled heating can be generated, in a very short time scale, on a defined electrode surface area. This localized heating is supposed to be similar to that could occur from a cell internal short-circuit (nail test).

The behavior of electrodes under laser pulses has been followed by both video and IR camera. Very specific and different reaction propagation mechanisms have been observed in function of the laser power and of the positive or the negative electrode definitions.

3.8. Propagation phenomenon

The laser power is high enough to start degradation reactions on charged electrodes. However, there is a fundamental difference between starting of the degradation reactions and propagation of initiated reactions.

The propagation speed is function of conductivity and specific heat of the electrodes, but also of thermal exchanges between electrode and its environment.

We have to consider the "heat balance", between the generated energy, the energy lost by convection, and the energy dissipated inside the electrode. As propagation phenomena are very rapid, we can consider that the energy lost by convection is negligible (around 20 J/s for all the electrode surface).

As a result, the propagation phenomenon is a function of pristine thermal stability of the studied charged electrode and of intrinsic electrode conductivity. This last point is now under more details studies.

As a result, in a first time, we have tried to establish a link between the thermal stability of each component of studied negative and positive electrodes and the occurrence or not of self-propagation.

Four different cases must be considered:

- there is no propagation phenomena after laser impact;
- the propagation starts, but there is an auto-inhibition;
- there is a self-propagation on a part of the electrode;
- there is a total self-propagation all over the electrode.

Laser power threshold (intensity, time, impact surface) has allowed to discriminate electrodes in function of their thermal stability and their ability to lead or not to self-propagation.

3.9. Characterization of positive electrodes

All obtained results have been summarized in Tables 5 and 6.

First, one should have to notice, that the positive electrode state of charge has a big influence on obtained results.

In the case of a total self-propagation, there is an electrode breakage (disappearance of aluminum collector), important flames and smokes, and the reached front propagation temperature is very high, between 700 and 900°C, and more than 1200°C for flames. These observations are in good agreement with previous DTA results. Moreover, post-mortem analysis, performed on positive electrodes after laser tests, have demonstrated the reduction of active material at Ni metal state and the disappearance of aluminum collector.

Table 5
Laser initiated reaction results on charged positive electrode

Positive electrode: test number and active material nature	4/5A end charge voltage (V)	Total charged capacity (mAh/g)	Irreversible capacity (mAh/g)	Laser in pulse mode (beam diameter impact: $D = 10$ mm)				Observed phenomena		Front reaction kinetics (cm/s)	Electrode breakage and Ni, Co metal
				I (mA)	P'_0 (W)	t (ms)	E'_0 (J)	Propagation	Flames § smokes		
Test a: $LiCoO_2$	4.20	155	10	10	360	500–1000	180–360	Very weak propagation and auto inhibition	Weak and localized	0.35	Not observed
Test b: $LiCoO_2$	4.35	175	10	10	360	500–1000	180–360	Very weak propagation and auto inhibition	Weak and localized		Not observed
Test c: $LiNi_{1-x}Co_xO_2$	4.00	180	40	10	360	300	110	Very strong propagation and electrode breakage	Strong	0.70	Yes
Test d: $LiNi_{1-x-y}Co_xM1_yO_2$	4.05	90	35	10	360	300–400	110–145	Strong propagation and electrode breakage	Strong	0.55	Yes
Test e: $LiNi_{1-x-y}Co_xM2_yO_2$	4.05	170	15	10	360	1000	360	Very weak propagation and auto inhibition	Weak and localized	0.55	Localized
Test f: $LiNi_{1-x-y-z}Co_xM1_yM2_zO_2$	4.20	190	40	10	360	800–900	290–325	Partial propagation and electrode breakage	Average		Localized

Table 6
Laser initiated reaction results on charged negative electrode

Negative electrode: test number and carbons type	4/5A end charge voltage (V)	Total charged capacity (mAh/g)	Laser in pulse mode (beam diameter impact: $D = 6$ mm)				Observed phenomena		Front reaction kinetics (cm/s)	Reached front temperature (°C)
			I (mA)	P'_0 (W)	t (ms)	E'_0 (J)	Propagation	Flames § smokes		
Test g: carbon type 1	4.10	240	10	360	500–800	180–290	Partial propagation and auto inhibition	Initial flash, no flame Smokes	0.40	≈450
Test h: carbon type 1	4.20	270	10	360	500–900	180–325	Partial propagation and auto inhibition	Initial flash, no flame Smokes		≈500
Test i: carbon type 2	4.00	240	10	360	200–300	75–110	Total propagation all over the electrode	Initial flash, no flame Smokes		≈500
Test j: carbon type 2	4.10	270	10	360	200–300	75–110	Total propagation all over the electrode	Initial flash, no flame Smokes	1.20	≈600

It not has been possible to initiate total self-propagation on charged $LiCoO_2$-based electrode, even at high state of charge (4.35 V). This result can be linked to the high thermal stability of $LiCoO_2$, in the whole (20–1000°C) temperature range, as previously demonstrated by X-ray diffraction experiments (Table 4). As the delithiated cobalt material is stable, even at high temperature, reaction with electrolyte, but particularly with PVDF binder, additive carbons and aluminum collector are reduced, and there is not enough local heat generation to entail propagation of reactions.

As doped nickel materials are less stable in the involved temperature range (20–1000°C, Table 4), it is more easy to initiate total self-propagation on corresponding electrodes, because of strong local heat generation. As previously demonstrated, M1 and M2 doping have a benefice effect on safety, because of oxygen release delay. Moreover, one should have also to notice a trend to reduce and to inhibit self-propagation phenomena with M2 dopant.

3.10. Characterization of negative electrodes

Laser beam initiation have been performed on two types of negative electrodes, at two states of charge, with different active materials (carbons, type 1 and 2). No significant influence of negative electrode charge state has been demonstrated, except in terms of front temperature reactions (amount of intercalated lithium in the carbon). On the contrary, the nature of the involved carbons is very important, as we can observe partial or total self-propagation phenomena.

3.11. Characterization of both negative/positive electrodes

Laser beam initiations have been also realized on (negative electrode/separator/positive electrode) stack. It has been demonstrated that negative electrode propagation could entail positive electrode self-propagation.

4. Conclusions

The whole obtained results (DTA, DSC and laser experiments) allow a better nail tests results understanding.

The stability of a done charged positive electrode is function of, first, active material ability to release oxygen (reaction temperature range and kinetic), and second, of active material ability to react with other components of the positive electrode (PVDF, additive carbons and aluminum collector).

If reactions with PVDF and additive carbons could occur, there is high enough local heat generation to entail a self-propagation all over the electrode.

The following positive electrodes ''safe ranking'' can be so proposed:

$$LiNi_{1-x-y}Co_xM2_yO_2 > LiCoO_2 > LiNi_{1-x-y}Co_xM1_yO_2 > LiNi_{1-x}Co_xO_2$$

On the negative side, the choice of the active carbon is the main ''safe parameter'', especially if we consider that negative electrode self-propagation is able to entail positive electrode self-propagation.

In conclusion, a new technique for a better understanding of Li-ion cell safety has been investigated. Useful and complementary results to those obtained from DSC and DTA experiments have been obtained and successfully linked to Li-ion cell behavior during abusive tests. Influence of the successive reactions kinetics on the overall process has been particularly well evidenced.

Acknowledgements

The authors wish to thank USABC for financial support, and J.P. Boeuve, V. Dillay, M. Duboureau, D. Guereau and R. Charrier for their very useful technical help.

References

[1] K. Sekai, H. Azuma, A. Omaru, S. Fujita, H. Imoto, T. Endo, K. Yamamura, Y. Nishi, J. Power Sources 43 (1993) 241.
[2] T. Nagaura, K. Tozawa, Prog. Batteries Solar Cells 9 (1990) 209.
[3] J.R. Dahn, U. von Sacken, M.W. Juzkow, H. Al-Janaby, J. Electrochem. Soc. 138 (1991) 2207.
[4] M. Broussely, F. Perton, Ph. Biensan, J.M. Bodet, J. Labat, A. Lecerf, C. Delmas, A. Rougier, J.P. Pérès, J. Power Sources 54 (1995) 109.
[5] M. Broussely, J. Power Sources 81 (1999) 142–143.
[6] Y. Oishi, T. Abe, T. Nagaura, M. Watanabe, US Patent 4,943,497.
[7] J.R. Dahn, E.W. Fuller, M. Obrovac, U. von Sacken, Solid State Ionics 69 (1994) 265–270.
[8] Ph. Biensan, B. Simon, J.P. Pérès, A. de Guibert, M. Broussely, J.M. Bodet, F. Perton, J. Power Sources 81–82 (1999) 906–912.